

**2<sup>+</sup> excitation of the <sup>12</sup>C Hoyle state**

M. Freer,<sup>1</sup> H. Fujita,<sup>2</sup> Z. Buthelezi,<sup>3</sup> J. Carter,<sup>2</sup> R. W. Fearick,<sup>4</sup> S. V. Förtsch,<sup>3</sup> R. Neveling,<sup>3</sup> S. M. Perez,<sup>3</sup> P. Papka,<sup>5</sup> F. D. Smit,<sup>3</sup> J. A. Swartz,<sup>5</sup> and I. Usman<sup>2</sup>

<sup>1</sup>*School of Physics and Astronomy, University of Birmingham, Birmingham, B15 2TT, United Kingdom*

<sup>2</sup>*School of Physics, University of the Witwatersrand, Johannesburg 2050, South Africa*

<sup>3</sup>*iThemba LABS, P.O. Box 722, Somerset West 7129, South Africa*

<sup>4</sup>*Physics Department, University of Cape Town, Private Bag, Rondebosch 7700, South Africa*

<sup>5</sup>*Physics Department, University of Stellenbosch, Private Bag X1, Matieland 7602, Stellenbosch, South Africa*

(Received 24 January 2009; published 19 October 2009)

A high-energy-resolution magnetic spectrometer has been used to measure the <sup>12</sup>C excitation energy spectrum to search for the 2<sup>+</sup> excitation of the 7.65 MeV, 0<sup>+</sup> Hoyle state. By measuring in the diffractive minimum of the angular distribution for the broad 0<sup>+</sup> background, evidence is found for a possible 2<sup>+</sup> state at 9.6(1) MeV with a width of 600(100) keV. The implications for the <sup>8</sup>Be + <sup>4</sup>He reaction rate in stellar environments are discussed.

DOI: [10.1103/PhysRevC.80.041303](https://doi.org/10.1103/PhysRevC.80.041303)

PACS number(s): 21.10.Re, 25.70.Ef, 25.70.Mn, 27.20.+n

One of the mysteries of nuclear structure is the nature of the 7.65 MeV, 0<sup>+</sup> state in <sup>12</sup>C. Its existence is innately tied to that of organic life as it is the portal through which the most abundant isotope of carbon (<sup>12</sup>C) is synthesized. The existence of the state was originally proposed by Hoyle [1] to address the question as to the abundance of <sup>12</sup>C, which could only be accounted for if a resonance were to lie close to the Gamow window. The anthropic power of this argument was demonstrated when the state was discovered by Cook and co-workers [2] with precisely the predicted properties.

The structure of this state has, however, remained something of a mystery. What is known is that it must have an unusual nature, which is probably a well-developed 3 $\alpha$ -cluster structure. Evidence for this comes from several sources. First, it is known that the optimal conditions for the formation of clusters is that a state should lie close to the associated cluster decay threshold [3]; in the present instance, the Hoyle state lies just 375 keV above the 3 $\alpha$ -decay threshold. Shell model calculations, for example, those of Ref. [4], reproduce rather well the energy of the first 2<sup>+</sup> (4.44 MeV) excitation. However, in the region of the second 0<sup>+</sup> state (0<sub>2</sub><sup>+</sup>), the Hoyle state, there is a void in the calculations; the energy of this state cannot be reproduced. A similar conclusion is reached in the no-core shell model calculations [5]. Analysis of electron inelastic-scattering data [6,7] indicates that the Hoyle state has a volume some 3.4 times larger than the ground state. This larger volume reduces the overlap of the  $\alpha$  particles and may allow them to obtain their quasifree characteristics in something approaching an  $\alpha$ -particle gas or perhaps a bosonic condensate (BEC) [8]. This latter possibility is intriguing, as it would correspond to a new form of nuclear matter in which the bosonic nature of the  $\alpha$  particles would allow the constituents to all occupy the lowest energy level of the mutual interaction potential—unlike fermions. Fermionic molecular dynamics (FMD) calculations also find that the 7.65 MeV state has a similar structure [9].

From an experimental perspective, one key ingredient in pinning down the structural properties of the state is finding the location of its collective (2<sup>+</sup>) excitation. A state in which

the three  $\alpha$  particles are arranged in a linear fashion (3 $\alpha$  chain) would have a 2<sup>+</sup> excitation at 0.8 MeV above the 0<sup>+</sup> state [10]. On the other hand, BEC calculations predict an energy difference of 1.3 MeV [11], the FMD predict 2.3 MeV [9], and the separation is 1.6–2.8 MeV in generator-coordinate method (GCM) calculations [12]. For a state with a similar compact structure to the ground state, the difference would be  $\sim$ 4.4 MeV. Historically, the observation of the 2<sup>+</sup> state has proved to be extremely difficult, as it is expected to be only weakly populated in most reactions (due to the well-developed cluster structure). The state should be broad and exist in an excitation energy region dominated by other states, some of which are also very broad [13]. Some tentative evidence for the existence of a 2<sup>+</sup> state at  $E_x = 9$ –10 MeV has been proposed [14], though not widely accepted. To solve this problem, an experiment with high sensitivity is required together with a technique for suppressing the other <sup>12</sup>C excited states. Here we present the results of such a measurement, providing the first strong evidence for the existence of the 2<sup>+</sup> excitation of the Hoyle state.

The measurements were performed with a 66 MeV proton beam (25 nA) provided by the separated sector cyclotron (SSC) accelerator at iThemba LABS, South Africa. The beam was incident on a 1 mg/cm<sup>2</sup> natural carbon target. Additional measurements were made with 200 MeV protons and Mylar (containing oxygen and hydrogen) and <sup>13</sup>C targets. The inelastically scattered protons were detected in the K600 magnetic spectrometer, which was operated in the dispersion matched mode [15]. In this mode, high energy resolution is achieved—in the present case, 24 keV [full width at half maximum (FWHM)] in <sup>12</sup>C excitation energy for the 66 MeV beam energy ( $\sim$ 40 keV at 200 MeV). Measurements were performed at a number of spectrometer angles:  $\theta_{\text{lab}} = 10^\circ$ ,  $16^\circ$ , and  $28^\circ$  at 66 MeV and  $\theta_{\text{lab}} = 7^\circ$ ,  $10^\circ$ ,  $13^\circ$ ,  $16^\circ$ , and  $20^\circ$  at 200 MeV. The main focus of the analysis presented here is the high-statistics, high-energy-resolution data acquired at the lower beam energy. At the three angles, the resolution achieved is very similar. The focal plane of the spectrometer is instrumented with two wire planes with a 4 mm wire

pitch with individual time-to-digital converter (TDC) readouts for determining the horizontal location, followed by two plastic scintillators for  $\Delta E$ - $E$  particle identification. There is an additional measurement of the vertical location of the scattered protons. The TDC readout allows the drift times to be determined and thus ray-tracing to be performed, thus providing enhanced position sensitivity. The difference in horizontal position at the two planes allows the angle of the protons to be reconstructed (the angular acceptance of the spectrometer was limited to  $\pm 2^\circ$ ). The excitation energy calibration of the focal plane was taken from known  $^{12}\text{C}$  excited states.

In the excitation energy region of interest, the spectrum is complicated. At 280 keV above the decay threshold, the following states occur: the narrow (8.5 eV) 7.65 MeV,  $0^+$  Hoyle state; a 9.64 MeV,  $3^-$  state, which is listed as having a width of 34(5) keV [16]; a  $1^-$  state at 10.84 MeV ( $\Gamma = 315(25)$  keV); and the unnatural parity state listed as  $J^\pi = 2^-$  at 11.83 MeV [ $\Gamma = 260(25)$  keV] [16]. Underlying all of these is a very broad  $0^+$  state at  $\sim 10.3$  MeV with a width of 3000(700) keV. In particular, it is this very broad  $0^+$  state that masks all other contributions in this region and inhibits the search for any  $2^+$  excitation of the Hoyle state.

To suppress the very broad  $0^+$  contribution, a measurement was performed at a scattering angle that coincides with a diffractive minimum ( $\theta_{\text{lab}} = 16^\circ$ ) in the angular distributions measured for the 7.65 MeV  $0^+$  state [17,18]. Figure 1 shows the cross sections (calculated by normalizing to the elastic scattering yields) for the three angles measured for the 4.44 MeV  $2^+$ , 9.64 MeV  $3^-$ , and 7.65 MeV  $0^+$  states. These are compared with coupled-channels calculations (CCRC) using the FRESKO code [19] with a collective form factor and the potentials from Ref. [18]. The absolute differential cross sections have been normalized to the data, while the excitation of the  $0^+$  state was assumed to proceed via a two-step mechanism through the 4.44 MeV  $2^+$  and 9.64 MeV  $3^-$  states. Although the variation of the experimental yield across the  $\pm 2^\circ$  angular acceptance for the  $16^\circ$  data indicates that the  $\theta_{\text{lab}} = 16^\circ$  setting lies precisely at the diffractive minimum, the calculations reproduce the experimental trends reasonably well. As can be seen from Fig. 1, the data indicate that the  $0^+$  contribution is reduced by a factor of  $>5$  at the minimum compared with the measurements at  $10^\circ$  and  $28^\circ$ .

The excitation energy spectrum for the full focal plane coverage at  $28^\circ$  is shown in Fig. 2. Here the states in  $^{12}\text{C}$  are marked above the axis together with peaks corresponding to contaminants in  $^{16}\text{O}$  (O) and  $^{13}\text{C}$  (C). The spectrometer was set up to focus reaction products from the  $^{12}\text{C}(p, p')$  reaction at a given excitation energy to a common point on the focal plane, i.e., to compensate for the reaction kinematics and momentum spread of the beam. Protons scattered off lighter and heavier masses have differing kinematics and are not focused in the same manner. A plot of focal plane position versus focal plane angle reveals locii whose focal plane positions depend on the focal plane angle and can be identified as originating from target contaminants. Measurements with a blank target frame (sensitive to the beam halo) indicate a flat spectrum at the level of 3 counts/keV, and this has been subtracted from the spectrum shown. The broad  $0^+$  state above the 7.65 MeV

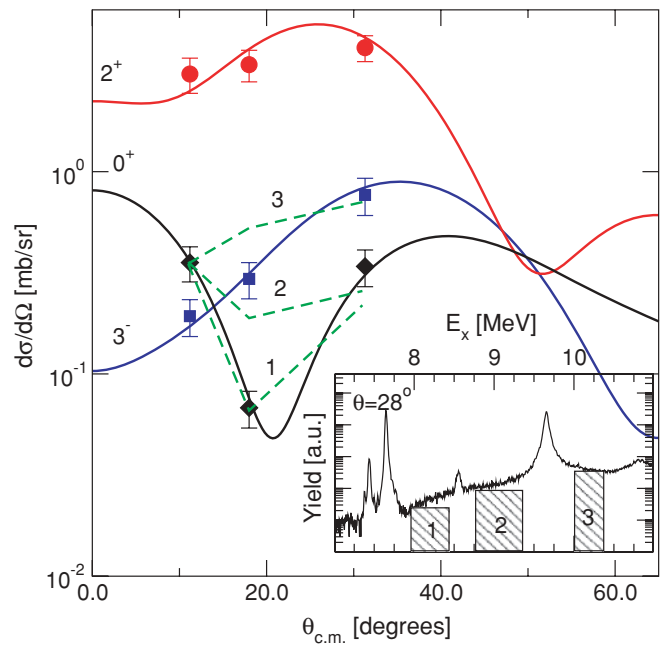


FIG. 1. (Color online) Differential cross sections for the population of states in  $^{12}\text{C}$  excited in the  $^{12}\text{C}(p, p')$  reaction at 66 MeV. The red circles, blue squares, and black diamonds correspond to the measured cross sections for the 4.44 MeV ( $2^+$ ), 9.64 MeV ( $3^-$ ), and 7.65 MeV ( $0^+$ ) states, respectively. The red, blue, and black curves correspond to CCRC calculations [19] of the angular distributions for the 4.44 MeV ( $2^+$ ), 9.64 MeV ( $3^-$ ), and 7.65 MeV ( $0^+$ ) states, respectively. The three sets of dashed lines show the yields (normalized to the  $0^+$  data point for  $\theta_{\text{c.m.}} = 11^\circ$ ) for the three regions of  $^{12}\text{C}$  excitation energy shown in the inset (see the main text for full discussion).

state is clearly seen as is the effect of the interference between the two  $0^+$  states found in the  $\beta$ -decay studies [13]. To determine the experimental excitation energy resolution, a Gaussian fit has been made to the 7.65 MeV peak resulting in a 24 keV FWHM. It should be noted that this resolution is achieved across the whole focal plane (e.g., the resolution of the 4.4 MeV state is 23 keV). An analysis of the  $3^-$  state indicates a width of 42(3) keV, significantly larger than the presently accepted value of 34(5) keV.

If a broad  $2^+$  component exists, then it should be most apparent at  $\theta_{\text{lab}} = 16^\circ$ . A comparison of the measured spectra at the three scattering angles is displayed in Fig. 3. The yields have been normalized to the area of the 7.65 MeV  $0^+$  peak. In each case, a flat background indicated by the blank target measurements of 3, 5, and 28 counts/keV at  $28^\circ$ ,  $16^\circ$ , and  $10^\circ$ , respectively, has been subtracted. The background subtraction yields spectra that have close to zero counts at 7.4 MeV (indicating it has been performed correctly). It should be noted that the background subtraction does not substantially affect the analysis of the data above the Hoyle state. Figure 3 shows that between 9 and 11 MeV, there is a significantly different spectral shape for the  $16^\circ$  data compared with the other two angles (note that the angular distribution for the 10.3 MeV state should follow that of the 7.65 MeV data). All three curves agree in amplitude close to 8.4 MeV, indicating that the  $0^+$  strength

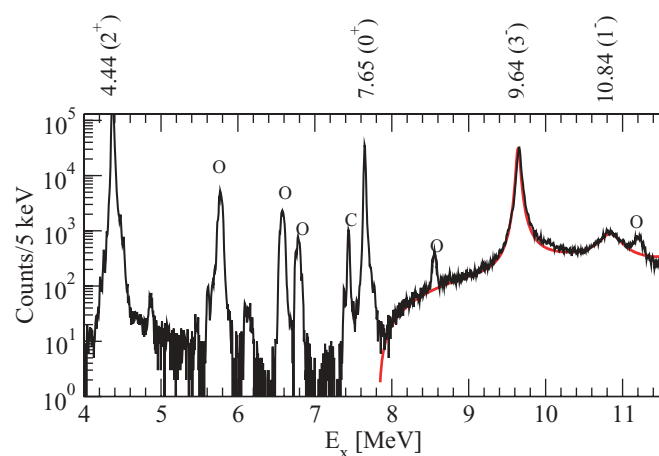


FIG. 2. (Color online)  $^{12}\text{C}$  excitation energy spectrum measured at  $\theta_{\text{lab}} = 28^\circ$ . Contaminants from  $^{16}\text{O}$  (O) and  $^{13}\text{C}$  (C) are indicated. The red line corresponds to line shapes including the broad 10.3 MeV  $0^+$ , 10.84 MeV  $1^-$ , and 11.83 MeV  $2^-$  states, i.e., without an additional  $2^+$  contribution included.

is the dominant contribution at this excitation energy. There is agreement across the range of excitation energies in the  $10^\circ$  and  $28^\circ$  data, indicating, as expected, that at these angles it is the broad  $0^+$  state that dominates. The  $16^\circ$  data give a clear indication of an extra component above 9 MeV.

To attempt to characterize the enhancement observed in Fig. 3, the  $16^\circ$  spectrum has been compared with peak components corresponding to the 9.64 ( $\Gamma = 42$  keV), 10.84, and 11.83 MeV states. The extraction of the broad  $0^+$  strength is complicated. Here, the  $0^+$  line shape was extracted from the

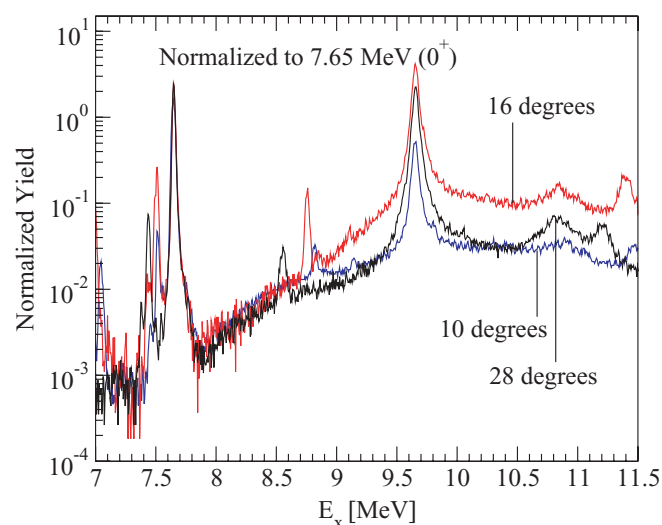


FIG. 3. (Color online) Three excitation energy spectra measured at  $\theta_{\text{lab}} = 10^\circ$  (blue),  $16^\circ$  (red), and  $28^\circ$  (black). The three spectra have been normalized to the area of the 7.65 MeV  $0^+$  peak. The continuum part of the data at  $10^\circ$  and  $28^\circ$  has approximately the same magnitude, whereas the  $16^\circ$  data show an enhancement close to 9.6 MeV, which is evidence for an additional component in the excitation energy spectrum.

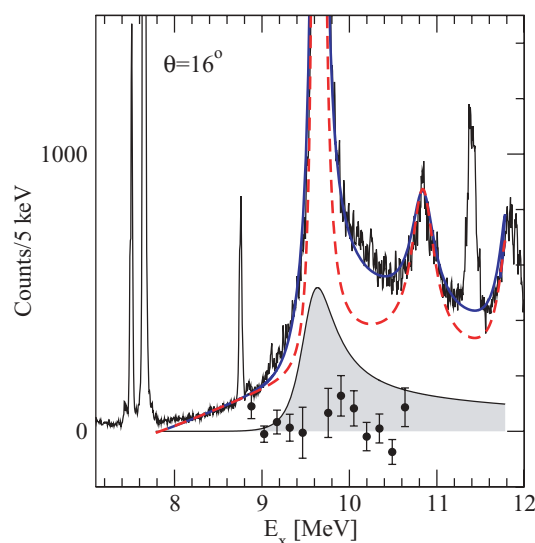


FIG. 4. (Color online)  $16^\circ$  data. The blue solid line and red dashed lines correspond to line shapes with and without the  $2^+$  contribution included. In both cases, the broad  $0^+$  strength is fixed by the yield at 8.4 MeV and the strengths of the peaks at 9.64, 10.84, and 11.83 MeV adjusted to fit the data. Note that the curve that omits the assumed  $2^+$  strength does not fit the data. The shaded region corresponds to the  $R$ -matrix-generated  $2^+$  line shape. The data points with associated error bars correspond to the calculated excess yield between 8.8 and 10.6 MeV from  $^{16}\text{O}$  contaminants in the target from measurements with carbon and Mylar targets at 200 MeV. The background strength does not account for the observed excess yield in the present data.

$10^\circ$  data. In this way, it also includes the known interference with the 7.65 MeV state. This line shape is also found to reproduce the data at  $28^\circ$  (Fig. 2). In Fig. 4, this has been normalized to the region around  $E_x = 8.4$  MeV (as suggested by Fig. 3). As expected from Fig. 3, these components do not describe the data above 9 MeV. The second line shape, which does fit the data well, includes an additional component of an  $R$ -matrix prediction for a 600 keV wide  $2^+$  resonance located at 9.6 MeV. As the resonance is located close to the  $L = 2$  centrifugal barrier, it has a rather asymmetric shape. This additional component produces a good description of the data. Figure 1 also shows the angular dependence of the yield for three parts of the  $^{12}\text{C}$  excitation energy spectrum, labeled 1–3. In region 1, the trend follows that of the 7.65 MeV state. In regions 2 and 3, the minimum in the angular distributions is less evident, indicating an additional component with a different spin. These three analytical approaches all indicate that the data are not described by known components.

A further important question is whether there are backgrounds that can describe the broad features in the present data. From an analysis of the correlations between the detection angle and position at the focal plane, it is possible to eliminate contributions from narrow states that are not kinematically corrected, e.g., elastic scattering from hydrogen in the target. Inelastic scattering from the  $^{13}\text{C}$  target shows that the peak close to  $E_x = 7.5$  MeV arises from the 7.55 MeV,  $5/2^-$  state. All other contributions at higher excitation energy were smaller by a factor of 10 (i.e., too small to account for

the present feature). There is a broad state known in  $^{13}\text{C}$  at 8.2 MeV [ $\Gamma = 1100(300)$  keV]. This would be located at 8.16 MeV, i.e., the wrong energy. Hence, the structure cannot be explained in terms of  $^{13}\text{C}$  contaminants. The second possibility is a reaction from  $^{16}\text{O}$  within the target. There is evidence for such contaminants, e.g., the peak at  $\sim 8.7$  MeV which corresponds to the 8.87 MeV,  $2^-$  excitation. The broad [ $\Gamma = 420(20)$  keV]  $^{16}\text{O}$  state at 9.59 MeV ( $J^\pi = 1^-$ ) would lie at  $E_x(^{12}\text{C}) = 9.46$  MeV at  $\theta_{\text{lab}} = 16^\circ$ . This state can be eliminated on a number of grounds: (i) the width is inconsistent, (ii) it could only describe the enhanced yield on the lower side of the  $^{12}\text{C}$  9.64 MeV peak (as seen in Fig. 3), and (iii) the angular distribution would follow that of the  $1^-$  state at  $E_x(^{16}\text{O}) = 7.11$  MeV; the  $1^-$  yield follows closely that of the  $3^-$  (found for the 7.11 MeV state), and thus in Fig. 3 the enhancement seen in the  $16^\circ$  data should appear in the  $28^\circ$  data—it does not. Finally, (iv) there is no evidence for such a contribution from reactions from the mylar target. The calculated excess yield from  $^{16}\text{O}$  contaminants in the target from measurements has been performed with carbon and Mylar targets at 200 MeV. The result is shown in Fig. 4. At 200 MeV, the 9.59 MeV ( $J^\pi = 1^-$ ) state should lie at 9.2 MeV. There is no evidence for any significant contribution. Finally, the peak cannot be described by final states such as  $3\alpha + p$  resulting from the decay of  $^5\text{Li}$  or  $^9\text{B}$ . In conclusion, there are no known contaminants that can describe the present data.

The data show a possible  $2^+$  resonance at 9.6(1) MeV with a width of 600(100) keV. It is interesting to compare this width with that of the 9.64 MeV  $3^-$  state. The penetrability for the  $3^-$  state decaying to the  $^8\text{Be}$  ground state is a factor of 4 to 4.5 times lower than for a  $2^+$  state, depending on the channel radius. Scaling the measured 42 keV by 4.5 would indicate a width for a  $2^+$  state of 190 keV. This is a factor of 3 less than that found here. The Wigner limit for the reduced width ( $\gamma_{\alpha W}^2 = 3\hbar^2/2\mu R^2$ ) indicates the maximum value of the width if the  $\alpha$  particle is preformed. This would correspond to a width for the state of 830 keV. The present width exhausts a large fraction (72%) of the Wigner limit indicating a large cluster content. The  $3^-$  state has a 7% decay branch to the  $^8\text{Be}(2^+)$  state [16], for a  $2^+$  state this could be up to a factor of 2 larger. This could also increase the width of the state a little. As this state could also have a well-developed cluster structure, it is thus natural to link the present resonance to the Hoyle state.

A  $2^+$  state at 9.6 MeV would, after 50 yr of speculation, finally exclude the existence of the  $3\alpha$ -chain state. The energy

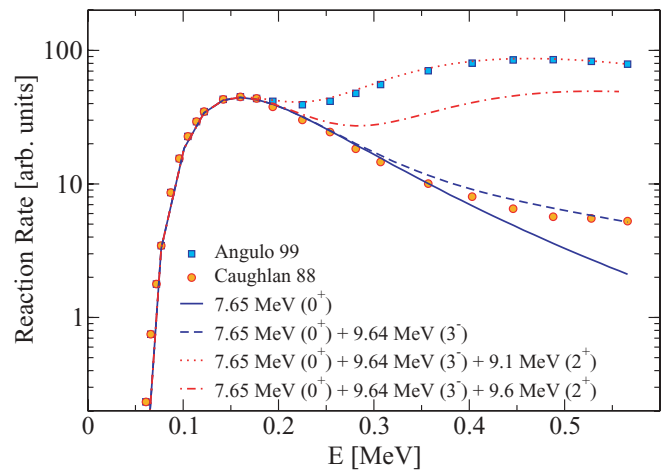


FIG. 5. (Color online) Calculated  $^4\text{He} + ^8\text{Be}$  reaction rates as a function of energy for different scenarios. The symbols correspond to the rates from the tabulations of Angulo [20] and Caughlan [21]. The lines correspond to the rates calculated for different contributions.

separation with respect to the 7.65 MeV state is  $\sim 2$  MeV making it consistent with the FMD and BEC calculations and far from the type of structure associated with the ground state. It would confirm the rather loosely bound  $\alpha$ -gas-like structure predicted by both these models.

Finally, Fig. 5 shows the influence of a  $2^+$  state on the  $^8\text{Be} + ^4\text{He}$  stellar reaction rate. Two compilations of this rate exist: Angulo [20] includes a  $2^+$  state at 9.1 MeV and in Caughlan [21] the state is omitted. We have calculated, using the formalism in Ref. [20], the impact of a  $2^+$  state at 9.6 MeV with an electromagnetic decay width as assumed in Ref. [20] (given the structure of this state, this width may be an overestimate). An enhancement of 5–10 is calculated for energies associated with explosive burning stellar scenarios.

Using a high-energy-resolution magnetic spectrometer, we found evidence for the possible existence of the  $2^+$  excitation of the Hoyle state at 9.6(1) MeV with a width of 600(100) keV. The separation of the state from the  $0^+$  Hoyle state is consistent with models that describe the structure of this excitation in terms of a loose arrangement of  $\alpha$  particles, i.e., an  $\alpha$ -gas-like state.

We are indebted to H. G. Bohlen (HMI) for the use of the  $^{13}\text{C}$  targets and to the skill of the accelerator staff.

[1] F. Hoyle, *Astrophys. J. Suppl. Ser.* **1**, 121 (1954).  
 [2] C. W. Cook *et al.*, *Phys. Rev.* **107**, 508 (1957).  
 [3] K. Ikeda *et al.*, *Prog. Theor. Phys. Suppl.*, **Extra Number**, 464 (1968).  
 [4] S. Karataglidis, P. J. Dortmans, K. Amos, and R. de Swiniarski, *Phys. Rev. C* **52**, 861 (1995).  
 [5] P. Navrátil, J. P. Vary, and B. R. Barrett, *Phys. Rev. Lett.* **84**, 5728 (2000).  
 [6] I. Sick and J. S. McCarthy, *Nucl. Phys.* **A150**, 631 (1970); A. Nakada, Y. Torizuka, and Y. Horikawa, *Phys. Rev. Lett.* **27**, 745 (1971); **27**, 1102(E) (1971); P. Strehl and Th. H. Schücan, *Phys. Lett.* **B27**, 641 (1968).

[7] Y. Funaki *et al.*, *Eur. Phys. J. A* **28**, 259 (2006).  
 [8] A. Tohsaki, H. Horiuchi, P. Schuck, and G. Ropke, *Phys. Rev. Lett.* **87**, 192501 (2001).  
 [9] M. Chernykh, H. Feldmeier, T. Neff, P. von Neumann-Cosel, and A. Richter, *Phys. Rev. Lett.* **98**, 032501 (2007).  
 [10] A. C. Merchant and W. D. M. Rae, *Nucl. Phys.* **A549**, 431 (1992).  
 [11] Y. Funaki, A. Tohsaki, H. Horiuchi, P. Schuck, and G. Ropke, *Phys. Rev. C* **67**, 051306(R) (2003).  
 [12] P. Descouvemont and D. Baye, *Phys. Rev. C* **36**, 54 (1987).  
 [13] H. O. U. Fynbo *et al.*, *Nature* **433**, 136 (2005).  
 [14] M. Itoh *et al.*, *Nucl. Phys.* **A738**, 268 (2004).

- [15] H. Fujita *et al.*, Nucl. Instrum. Methods **A484**, 17 (2002).  
[16] F. Ajzenberg-Selove, Nucl. Phys. **A506**, 1 (1990).  
[17] G. R. Satchler, Nucl. Phys. **A100**, 497 (1967).  
[18] S. Chiba *et al.*, Nucl. Sci. Tech. **37**, 498 (2000).  
[19] I. J. Thompson, Comput. Phys. Rep. **7**, 167 (1988).  
[20] C. Angulo *et al.*, Nucl. Phys. **A656**, 3 (1999).  
[21] C. R. Caughlan and W. A. Fowler, At. Data Nucl. Data Tables **40**, 283 (1988).